

S5-013

Structural characterisation of the photosystem two reaction centre from *Synechococcus elongatus* using electron microscopy and single particle analysis.

JL Duncan, J Nield and J Barber

Wolfson Laboratories, Department of Biochemistry, Imperial College of Science Technology and Medicine, London SW7 2AY, UK. j.barber@ic.ac.uk, Tel, +44(0)207 594 5266 Fax +44(0)207 594 5272.

Keywords: Photosystem two, 3D Structure, electron microscopy, single particle analysis, extrinsic proteins.

Introduction

It has previously been shown that photosystem II (PSII) can be isolated from higher plants (spinach) and cyanobacteria (*Synechococcus elongatus*) as a dimeric core complex (Boekema et al 1995). In both cases the dimeric complexes had lost their outer light harvesting systems; LHCII/CAB proteins and phycobilisomes for higher plants and cyanobacteria, respectively. From negative stain electron microscopy (EM) the dimensions of these core dimers were measured to be 220 Å x 150 Å with a height of 95 Å (Nield et al. 2000, Nield et al. 1998). According to size exclusion chromatography the molecular masses of the core dimers are estimated to be about 450 kDa and they bind approximately 32 chlorophylls per reaction center (Zouni et al. 2001). It therefore seems that this basic structural unit is maintained between higher plants and cyanobacteria although the reason for the dimeric conformation is unclear. One possibility is that it helps to maintain the stability of the PSII complex even after photoinduced damage has occurred in the D1 reaction centre protein (Kruse et al. 1997). Thus the degradation and replacement of the damaged D1 protein can only occur when the dimer undergoes monomerisation (Barbato et al. 1992).

Although the dimeric nature of the PSII complex seems to be a common feature shared between higher plants and cyanobacteria there are differences in some other aspects of their structure. The docking of the phycobilisome to the stromal surface of cyanobacterial PSII cores contrasts with the hydrophobic attachment of the LHCII and other CAB proteins to the side of the higher plant dimer. Moreover, although both types of PSII bind the 33 kDa PsbO protein of the oxygen evolving complex (OEC) to their luminal surface, the PsbP and PsbQ proteins in higher plants are replaced by the PsbU and PsbV proteins in cyanobacteria.

Despite these differences it is usually assumed that cyanobacteria can be a meaningful model system for higher plants, an argument that is sustained by the large volume of mutational studies conducted on the transformable cyanobacterium *Synechocystis* PC6803 (Putnam-Evans et al. 1996). Similarly the thermophilic cyanobacterium *S. elongatus* has provided highly stable and active PSII preparations suitable for in depth biophysical (Schatz & Witt 1984.) and structural studies. Indeed, 3D crystals and X-ray structures have been obtained of PSII (Zouni et al. 2001) as well as PSI (Jordan et al. 2001) of this organism. Recently, EM coupled with single particle analyses was used to obtain the first 3D structural model of the PSII core dimer from *S. elongatus* after negative staining (Nield et al. 2000). Here we extend this work to the calculation of a 3D model for the PSII dimeric core of *S.*

elongatus using electron cryo microscopy. In so doing we have improved the resolution of the model from 30 Å to 17 Å and further characterized the structural features and positioning of the OEC proteins.

Materials and Methods.

Isolation of oxygen evolving dimeric PSII core complexes from *Synechococcus elongatus* - PSII cores were isolated as previously described (Nield et al. 2000) from the thermophilic cyanobacterium *S. elongatus*.

Electron microscopy and densitometry - The PSII dimer sample was imaged in vitreous ice (Dubochet et al. 1988) at liquid nitrogen temperature using a Philips CM200 FEG EM at a calibrated magnification of 48,600x. 32 micrographs consisting of 16 focal pairs, where the first micrograph of a focal pair was calculated to have been imaged at ~1.8 µm under focus, with the second image further from focus at ~3.2 µm. These micrographs were specifically chosen given their minimal astigmatism, drift and appropriate particle concentration. They were subsequently digitised locally using a Leaf Scan 45 densitometer at a step size of 10 µm, thus yielding a sampling interval of 2.0576 Å per pixel on the specimen scale.

Image processing - All image processing routines were carried out using the IMAGIC-5 software environment (van Heel et al, 1996). Single particles were interactively selected from the more under-focused micrograph of each focal pair and floated into 192 x 192 pixel boxes. The co-ordinates of the selected particles were then used to extract particles from the closer to focus micrograph. After correcting for the Contrast Transfer Function (CTF), the merging of images from the two different defoci led to an increase in the uniformity of the spatial frequency distribution. Two separate data sets were built, each of ~3000 particles, from the closer and further from focus micrographs. A locally developed program “dsload”, gratefully supplied by Dr E. Morris, was used to aid in the accurate determination of the CTF by inspection of the 2D Fast Fourier Transform (FFT) calculated on a per micrograph basis. A series of masks were then constructed, down to an 8 Å limit, to allow for correction of the phase component of the CTF. The pre-treated images were initially aligned using reference-free procedures (Schatz et al. 1995). Class averages from this initial procedure were then used as references for the first round of multi-reference alignment. Multi-variate statistical analysis was employed as described previously (Schatz et al. 1995) and the procedure iteratively refined, resulting in 86 improved class averages taken forward for angular reconstitution (van Heel et al. 1987). An initial 3D reconstruction was obtained as a starting point from which 2D reprojections were calculated and used to search the data set for novel views and aid subsequent angular assignment. Several sub-populations of particles were identified and processed independently. These yielded a number of 3D models differing in point group symmetry e.g. single dimers (C2 point group symmetry) and double dimers (D2). The entire original data set was searched using 2D reprojections from these 3D models in order to further refine the sub-populations identified. The largest sub-population identified ~2500 molecular images of the single dimer, which also displayed the most luminal density observed. This was selected for further iterative refinement (Schatz et al. 1995) resulting in the final 3D model presented.

Resolution was determined by Fourier Shell Correlation, compensated for the C2 point group symmetry (Orlova et al. 1997).

Results.

Figure 1A shows three typical class averages of a total of 86 used to reconstruct the final 3D map in Fig 1C viewed at the same orientation as the class averages shown. Figure 1B are the corresponding reprojections from the 3D model. The Fourier Shell Correlation Function

(FSCF) for the refined 3D map is displayed in Fig 1D. The 3σ curve crossed the FSCF at 0.06 which yields approximately 17\AA . Figure 2 is a comparison between the surface rendered view derived from the Cryo EM 3D reconstruction and the 3D surface representation of the model of *S.elongatus* core dimer obtained by X-ray crystallography (Zouni et al 2001). Both maps have similar overall dimensions with the Cryo 3D EM map having dimensions of $190\text{\AA} \times 120\text{\AA}$ with a height of 105\AA . However, there seems to be differences in density distribution associated with the extrinsic luminal proteins

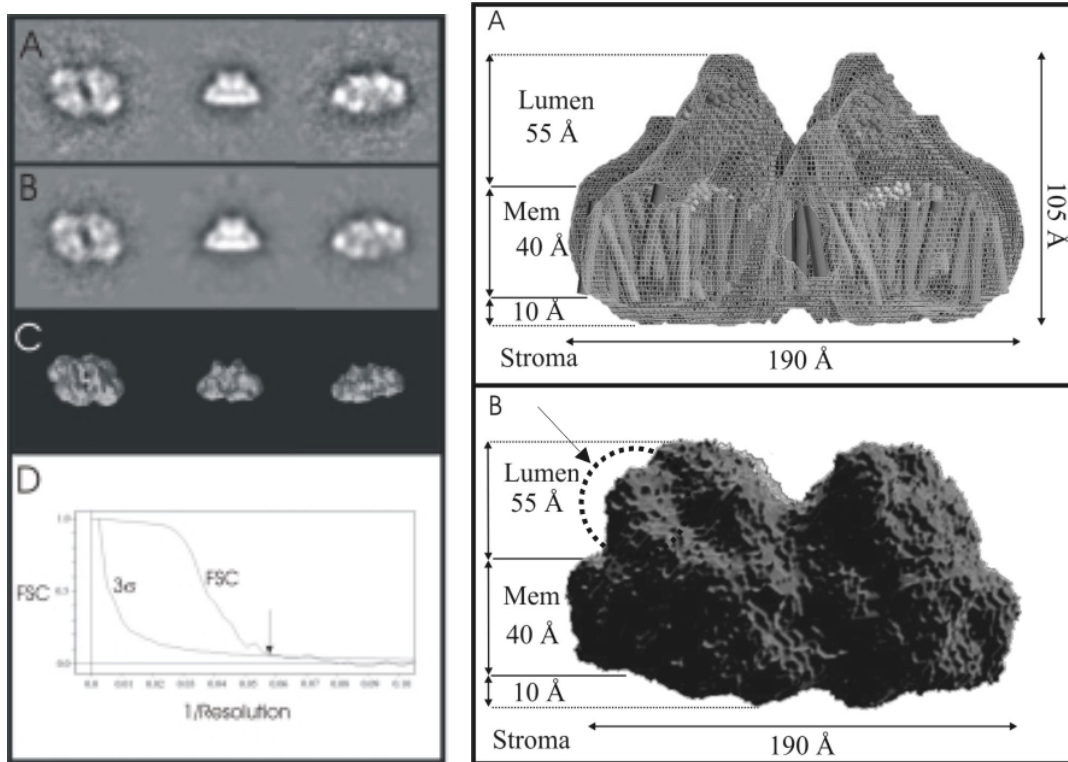


Figure 1. Figure 1A shows three of the 86 class averages, calculated from a data set of 2500 CTF corrected molecular images, used to build the 3D cryo model. Figure 1B highlights the corresponding reprojected views from the 3D model. 1C displays the surface rendered 3D model in the appropriate orientations. 1D shows the Fourier Shell Correlation Function for the 3D Cryo map and a 3σ curve. The 3σ curve crosses at approximately $1/0.06 = \sim 17\text{\AA}$.

Figure 2 A comparison between the molecular envelope of the PSII homodimer, achieved from our cryo electron microscopy and single particle analysis, and the 3D crystal X-ray diffraction data (adapted from Zouni et al 2001). Figure 2A highlights the surface of the PSII homodimer into which the X-ray helices have been modelled. The overall dimensions for this complex are 190\AA long, 105\AA high, including the luminal extrinsic domain, and 120\AA deep.

Discussion.

Although the single particle analysis of the isolated PSII dimeric core of *S. elongatus* presented here is overall consistent with the structure of the same complex derived by X-ray crystallography, there are some important differences. The intrinsic portion of the EM derived 17 Å map readily accommodates the transmembrane helices identified by Zouni et al 2001. The main difference between the maps is seen in the distribution of density at the luminal surface. The X-ray data gave a cylindrical-shaped density of 35 Å length, which was composed of β-strand that protrudes at 45 degrees to the membrane plane (see arrow Fig 2B). It was suggested that this density corresponded to about one half of the PsbO protein. This feature was not seen in our 3D model derived by single particle analysis. Instead the density we attribute to the PsbO protein lays along the luminal surface, a conclusion also drawn from similar single particle analyses of the PSII supercomplex from higher plants (Nield et al, 2001). In both cases the density assigned to the PsbO protein is about 80 Å long and 20 Å wide and is positioned across the luminal ends of the helices of the D1 and D2 proteins and helices 5 and 6 of CP47.

A possible explanation for the difference between the EM and X-ray models may stem from the fact that it is known that the PsbO is an elongated, flexible protein, which seems to have a centrally located hinge region (De Las Rivas and Heredia, 1999). Mutational and modelling studies indicate that the N-terminus of the PsbO is a docking region interacting with the large extrinsic luminal loop of CP47, while the C-terminal half is more flexible. It is therefore possible that the 45 degree protrusion observed in the X-ray structure is the C-terminal half of the PsbO protein which has adopted a non-physiological conformation within the crystal. Indeed, this protein mass plays an important role in making contacts between adjacent complexes within the 3D crystal lattice. Therefore, our suggestion that the PsbO protein lays along the surface of the complex may be a more true representation of its physiological conformation.

References.

- Barbato R et al. (1992) *J. Cell Biol.* **119** 325-335.
[Boekema EJ et al \(1995\)](#). *Proc Natl Acad Sci U S A.* **92** 175-9.
 De Las Rivas, Heredia P. (1999) *Photosynthesis Research* **61** 11-21.
[Dubochet J et al.](#) (1988) *Q Rev Biophys* **21** 129-228.
[Jordan P et al.](#) (2001) *Nature.* **411** 909-17.
[Kruse O, Zheleva D, Barber J.](#) (1997) *FEBS Letts.* **408** 276-80.
 Nield J et al. (1998) *In: Proceedings of the 14th International Congress on Electron Microscopy*, **IV**:619-620
[Nield J et al.](#) (2000) *J Biol Chem.* **275** 27940-6.
 Nield J et al (2001) *In: Proceedings of the 12th International Congress on Photosynthesis*, Brisbane, Australia. *submitted*.
[Putnam-Evans C, Wu J, Bricker TM.](#) (1996) *Plant Mol Biol.* **32** 1191-5.
[Orlova EV et al.](#) (1997) *J Mol Biol.* **271** 417-37.
[Schatz GH & Witt HT.](#) (1984) *Photobiochem Photobiophys* **7** 1-14.
 Schatz M et al. (1995) *J Struct Biol.* **114** 28-40.
[van Heel M, Harauz G, Orlova EV.](#) (1996) *J Struct Biol.* **116** 17-24.
 van Heel, M. (1987) *Ultramicroscopy.* **21** 111-124
[Zouni A et al.](#) (2001) *Nature.* 2001 **409** 739-43.